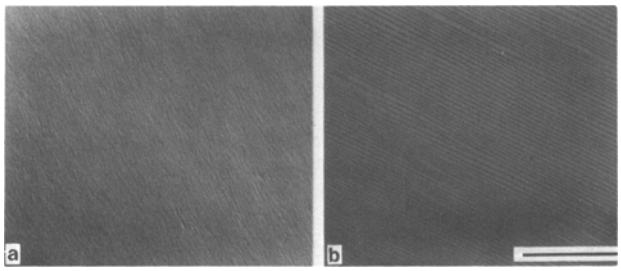

Fig. 8. Typical surface morphologies observed on (a) a back-melted InP substrate, and (b) a back-melted epi-layer. The marker represents 1.0 mm.

## Acknowledgments

The authors gratefully acknowledge the help of D. Brasen and J. A. Lourenco in different phases of the experiment and appreciate the comments of G. Y. Chin, J. V. DiLorenzo, and J. H. Wernick on the manuscript.

Manuscript received Oct. 9, 1981.

Any discussion of this paper will appear in a Discussion Section to be published in the June 1983 JOURNAL. All discussions for the June 1983 Discussion Section should be submitted by Feb. 1, 1983.

*Publication costs of this article were assisted by Bell Laboratories.*

REFERENCES

1. G. S. Stringfellow, *J. Appl. Phys.*, **43**, 3455 (1972).
2. G. H. Olsen, *J. Cryst. Growth*, **31**, 223 (1975).
3. P. M. Petroff and R. L. Hartman, *Appl. Phys. Lett.*, **23**, 469 (1973).
4. P. W. Hutchinson and P. S. Dobson, *Philos. Mag.*, **32**, 745 (1975).
5. K. Ishida, T. Kamejima, and J. Matsui, *Appl. Phys. Lett.*, **31**, 397 (1977).
6. S. Mahajan, W. D. Johnston, Jr., M. A. Pollack, and R. E. Nahory, *ibid.*, **34**, 717 (1979).
7. B. V. Dutt, S. Mahajan, R. J. Roedel, G. P. Schwartz, D. C. Miller, and L. Derick, *This Journal*, **128**, 1573 (1981).
8. M. Ettenberg, S. H. McFarlane, and S. L. Gilbert, Proc. of the 4th International Symposium on GaAs and Related Compounds, p. 23, Boulder, CO (1973).
9. G. A. Rozgonyi, P. M. Petroff, and M. B. Panish, *Appl. Phys. Lett.*, **24**, 251 (1974).
10. G. H. Olsen, M. S. Abrahams, C. J. Buiocchi, and T. J. Zamerowski, *J. Appl. Phys.*, **46**, 1243 (1974).
11. M. Ettenberg, C. J. Nuese, J. R. Appert, J. J. Gannon, and R. E. Enstrom, *J. Electron. Mater.*, **4**, 37 (1975).
12. S. N. G. Chu, S. Mahajan, K. E. Strege, W. D. Johnston, Jr., and A. A. Ballman, *Appl. Phys. Lett.*, **38**, 766 (1981).
13. R. H. Saul, *This Journal*, **118**, 793 (1971).
14. H. Temkin, V. G. Keramidas, and S. Mahajan, *This Journal*, **128**, 1088 (1981).
15. A. Huber and N. T. Linn, *J. Cryst. Growth*, **28**, 80 (1975).
16. S. Mahajan and A. K. Chin, *ibid.*, **54**, 138 (1981).
17. H. Queisser, *ibid.*, **17**, 169 (1972).
18. M. B. Small, R. Ghez, R. Potemski, and W. Reuter, *This Journal*, **127**, 1177 (1980).
19. K. Pak, T. Nishinaga, and S. Uchiyama, *Jpn. J. Appl. Phys.*, **16**, 949 (1977).

# Growth Kinetics of Silicon Thermal Nitridation

**Ching-Yuan Wu and Chwan-Wen King**

*Institute of Electronics, National Chiao-Tung University, Hsin-Chu, Taiwan, China*

**and Ming-Kwang Lee* and Chin-Tang Chen**

*IC Development Center, Electronics Research and Service Organization, Industrial Technology Research Institute, Hsin-Chu, Taiwan, China*

ABSTRACT

An analytic model for the growth kinetics of silicon thermal nitridation has been developed, in which the nitrogen radicals diffused across the as-grown thermal silicon nitride layer have been characterized by a characteristic diffusion length. It has been shown that the direct thermal nitridation of silicon in ammonia gas or nitrogen gas is similar to the silicon oxidation in oxygen or steam when the characteristic diffusion length of the nitrogen radicals is much larger than the as-grown silicon nitride layer. However, when the thickness of the as-grown silicon nitride film is larger than the characteristic diffusion length of the nitrogen radicals, the thickness of the as-grown silicon nitride film tends to saturate. The self-limiting growth has been verified to be the "logarithmic" relation of the developed model, and the activation energy of the quasi-saturation thickness has been shown to be the activation energy of the characteristic diffusion length. Based on comparisons between the experimental data and the developed model, the characteristic diffusion length has been shown to be very short and has been estimated to be smaller than 10Å for nitridation temperature below 1200°C, and its activation energy has been estimated to be of 0.181 eV. Moreover, the linear growth rate constant and the parabolic growth rate constant of the as-grown thermal nitride films have been estimated to be of 1.286 and 1.546 eV, respectively, which are smaller than those of the silicon oxidation in dry oxygen or steam ambient. In addition, it has been shown that the linear growth rate constant of the thermal nitridation using ammonia gas is larger than that of the thermal oxidation using dry oxygen or steam ambient, which predicts that the surface-limited reaction of the silicon surface in ammonia gas is faster than that in dry oxygen or steam ambient.

Silicon nitride films, which exhibit high structure density, high dielectric constant, good electrical properties, and strong inertness toward chemicals, have been widely used in semiconductor devices and integrated circuit fabrications. However, high quality silicon nitride films have been prepared by expensive methods such as chemical vapor deposition (CVD) or plasma deposition. In modern silicon technologies, thicker silicon diode films (>1000Å) with satisfactory quality and precise thickness can be easily obtained by the direct thermal oxidation of the silicon surface. However, thin silicon dioxide films (<500Å) with high quality and reproducible properties have become a challenge for the present technique. Before 1976, much effort was made to prepare the silicon nitride films by using the reaction of the silicon surface in nitrogen ambient; however, no continuous nitride films had been obtained (1-5). Until 1978, Fujitsu Laboratories

* Electrochemical Society Active Member.
Key words: diffusion, oxidation, silicon nitride.

Limited (6) had reported that continuous and uniform silicon nitride films could be obtained by the direct nitridation of the silicon surface in nitrogen or ammonia ambient. Later, thermally grown silicon nitride films for the gate insulator of the IGFET devices had been successfully fabricated (7), and the dielectric constant of the as-grown films was shown to be about 30% larger that that of the silicon dioxide films. Moreover, it had been shown that low surface state density and high electron mobility could be obtained for an n-channel MOSFET. It is believed that thermally grown silicon nitride films will be the important materials for device applications, especially for the gate insulator of future submicron MOS devices. However, no detailed reports on the growth kinetics of the as-grown thermal nitride films have been given. It has been shown (5, 6, 8) that the thermal nitridation of the silicon surface was quite different from the thermal oxidation of the silicon surface. In the case of thermal oxidation the growth kinetics can always be described by the expression, $X_o^2 + AX_o = B(t + \tau)$, where $X_o$ is the oxide thickness, $t$ is the oxidation time, $\tau$ is the initial oxide thickness, and $A$ and $B$ are the growth rate constants. The major difference between the thermal nitridation and the thermal oxidation is that the as-grown thermal nitride films have higher structure density, so "self-limiting" growth can easily occur for the thermal nitridation of the silicon surface in nitrogen or ammonia ambient. Although the growth kinetics of the as-grown thermal nitride films are not yet clear, this self-limiting growth property does become a unique advantage for some semiconductor devices in which thin insulator films with high quality and precise thickness are needed.

In this paper an analytical model for the thermal nitridation of the silicon surface has been developed to interpret the growth kinetics of the as-grown thermal nitride films at different nitridation temperature. Experimental results of the as-grown thermal nitride films using ammonia gas for nitridation temperature from 700° to 1200°C are given and compared with the developed model. Based on comparisons between the experimental results and the developed model, the growth rate constants and characteristic parameters of the thermal nitridation in ammonia gas have been first deduced. Moreover, discussions and conclusions are given.

## Growth Kinetics Model

There are three basic steps for the thermal nitridation of the silicon surface. These steps can be easily understood from Fig. 1. First, the nitridant species must be transported from the bulk of the ammonia gas to the thermal nitride-gas interface. Second, the nitridant species diffuse across the thermal nitride film. Third, the nitridant species react with the silicon surface. According to Fig. 1, the three fluxes corresponding to each step must be equal at each boundary. In region (I), the nitridant flux $F_1$ can be expressed by (7)

$$F_1 = h_G(C_G - C_S) \quad [1]$$

where $C_G$ is the concentration of the nitridant species in the ammonia ambient, $C_S$ is the concentration of the nitridant species at the thermal nitride-gas interface, and $h_G$ is the mass-transfer coefficient.

If we assume that Henry's law is valid, then the concentration at the outer surface of the thermal nitride $C_O$ is proportional to the partial pressure of the nitridant species next to the thermal nitride surface $P_S$, *i.e.*, $C_O = HP_S$, where $H$ is the Henry law constant. In addition, if we assume the equilibrium concentration of the nitridant species in the bulk of the ammonia gas to be $C^*$, then $C^*$ can be related to the partial pressure of the nitridant species $P_G$ by $C^* = HP_G$. According to the ideal gas law, $C_G = P_G/k_BT$ and $C_S = P_S/k_BT$, we may then rewrite Eq. [1] as

$$F_1 = h(C^* - C_O) \quad [2]$$

where $h$ is the gas phase mass-transfer coefficient in terms of concentrations in the solid, which is given by $h = h_G/Hk_BT$.

In region III, the reaction rate at the nitride-silicon interface, which is proportional to the concentration of the nitridant species at the interface $C_i$, can be expressed by

$$F_3 = k_s C_i \quad [3]$$

where $k_s$ is the chemical surface-reaction rate constant for thermal nitridation.

In region II, the flux of the nitridant species can be assumed to be a diffusive flux, and is expressed as

$$F_2(x) = -D_N \frac{dC(x)}{dx} \quad [4]$$

where $D_N$ is the diffusivity of the nitridant species in the thermal nitride film.

According to the continuity equation, we define a characteristic time constant $\tau_N$ for the nitridant species across the thermal nitride. We may then write the continuity equation as

$$\frac{\partial C(x,t)}{\partial t} = \nabla \cdot \vec{F}_2(x) + \frac{C(x,t)}{\tau_N} \quad [5]$$

For steady state, the diffusion equation for the nitridant species across the thermal nitride film can be written as

$$\frac{d^2C(x)}{dx^2} - \frac{C(x)}{L_N^2} = 0 \quad [6]$$

where $L_N = (D_N\tau_N)^{1/2}$ is the characteristic diffusion length for the nitridant species across the thermal nitride film.

Using the boundary conditions at $x = 0$ and $X_o$, *i.e.*, $C(0) = C_O$ and $C(X_o) = C_i$, Eq. [6] can be easily solved. The result is

$$C(X) = \frac{C_i \sinh\left(\frac{X}{L_N}\right) + C_O \sinh\left(\frac{X_o - X}{L_N}\right)}{\sinh\left(\frac{X_o}{L_N}\right)} \quad [7]$$

Since the flux must be continuous at each boundary, *i.e.*, $F_1 = F_2(x = 0)$, $F_3 = F_2(X = X_o) = -D_N \left.\frac{dC(x)}{dx}\right|_{x=x_o}$, the concentration of the nitridant species at the thermal nitride-silicon interface can be expressed in terms of $C^*$. The result is

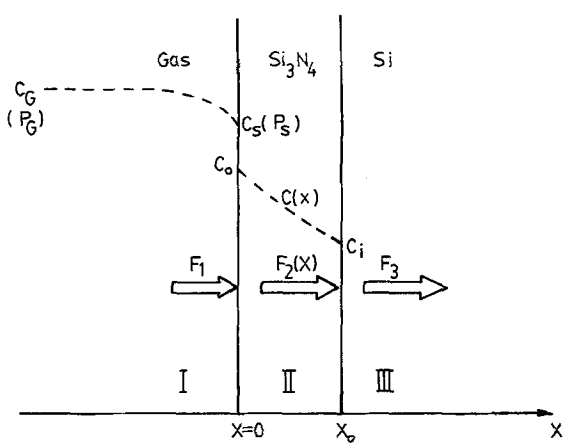


Fig. 1. Growth kinetics diagram of the thermal nitridation

$$C_i = \frac{C^*}{\left(\frac{k_s L_N}{D_N} + \frac{D_N}{L_N h}\right)\sinh\left(\frac{X_o}{L_N}\right) + \left(1 + \frac{k_s}{h}\right)\cosh\left(\frac{X_o}{L_N}\right)} \quad [8]$$

The flux of the nitridant species reaching the thermal nitride-silicon interface is given by

$$N_1 \frac{dX_o}{dt} = F_3 = F_2(X = X_o) = k_s C_i = \frac{k_s C^*}{\left(\frac{k_s L_N}{D_N} + \frac{D_N}{L_N h}\right)\sinh\left(\frac{X_o}{L_N}\right) + \left(1 + \frac{k_s}{h}\right)\cosh\left(\frac{X_o}{L_N}\right)} \quad [9]$$

where $N_1$ is the number of the nitridant species incorporated into a unit volume of the thermal nitride.

Solving Eq. [9] and assuming $X_o = 0$ for $t = 0$ we obtain

$$L_N A \sinh\left(\frac{X_o}{L_N}\right) + 2L_N^2\left[\cosh\left(\frac{X_o}{L_N}\right) - 1\right] = Bt \quad [10]$$

where $A$ and $B$ are separately defined as

$$A = \frac{2L_N\left(1 + \frac{k_s}{h}\right)}{\left(\frac{k_s L_N}{D_N} + \frac{D_N}{L_N h}\right)} \quad [11]$$

$$B = \frac{2L_N k_s C^*}{N_1\left(\frac{k_s L_N}{D_N} + \frac{D_N}{L_N h}\right)} \quad [12]$$

Note that Eq. [10] can be used to calculate $X_o$ in terms of $t$, and the result is

$$X_o = L_N \ln\left\{\frac{(2L_N^2 + Bt) + [(Bt)^2 + L_N^2A^2 + 4L_N^2Bt]^{1/2}}{2L_N^2 + AL_N}\right\} \quad [13]$$

The growth rate of the thermal nitride is then written as

$$\frac{dX_o}{dt} = L_N \left\{\frac{B + \frac{1}{2}[(Bt)^2 + L_N^2A^2 + 4L_N^2Bt]^{1/2}(2B^2t + 4L_N^2B)}{(2L_N^2 + Bt) + [(Bt)^2 + L_N^2A^2 + 4L_N^2Bt]^{1/2}}\right\} \quad [14]$$

There are two extreme cases that deserve further discussion. In the case of $X_o << L_N$, Eq. [10] can be simplified to

$$X_o^2 + AX_o = Bt \quad [15]$$

where $\sinh(X_o/L_N) \cong X_o/L_N$ and $\cosh(X_o/L_N) \cong 1 - \frac{1}{2}(X_o/L_N)^2$ are used in Eq. [10] to obtain Eq. [15].

From Eq. [15] it is clearly seen that when $X_o$ is very small and $X_o << L_N$, the surface reaction growth will be dominant, which is the same as the conventional oxidation of the silicon surface. In this case, the constants $A$ and $B$ can be reduced to the conventional expressions, *i.e.*,

$$A = 2D_N\left(\frac{1}{h} + \frac{1}{k_s}\right) \quad [16]$$

$$B = \frac{2D_N C^*}{N_1} \quad [17]$$

Similarly, two distinguished regions can also be classified. From Eq. [15], when $X_o << A$, we may obtain $X_o = \frac{B}{A}t$ where $\frac{B}{A}$ is referred to be the linear rate constant; when $X_o >> A$, we obtain $X_o = (Bt)^{1/2}$ where $B$ is the parabolic rate constant. Note that Eq. [15] is valid when the condition $X_o << L_N$ is satisfied, so the parabolic relationship may not exist if the diffusion length is very short.

In the case of $X_o >> L_N$, Eq. [10] or Eq. [13] can be simplified to

$$X_o = L_N \ln\left[\frac{Bt}{L_N^2 + \frac{A}{2}L_N}\right] \quad [18]$$

The growth rate in this case can be written as

$$\frac{dX_o}{dt} = \frac{L_N}{t} \quad [19]$$

It is clearly seen that the growth rate in this region is very small when the nitridation time is long and the diffusion length of the nitridant species across the thermal nitride layer is short. This region is called the "logarithmic region." Due to higher structure density of the as-grown thermal nitride films, the characteristic diffusion length is very small, so the logarithmic relationship can be easily accomplished for shorter nitridation time. That is why thermal nitridation has the property of "self-limiting" growth. Moreover, based on Eq. [19], the characteristic diffusion length of the nitridant species across the thermal nitride film can be deduced.

A typical plot of Eq. [13] is shown in Fig. 2 for reference. It is clear that $A$, $B$, and $L_N$ can be deduced by matching Eq. [13] and the experimental data if three regions can be clearly classified.

## Experimental Results and Discussion

Silicon p-type <100> oriented wafers were used as the starting materials. After degreasing in an organic solvent such as ACE and TCE, the wafers were boiled in sulfuric and nitric acids. Before loading into the quartz tube, the cleaned wafers were dipped into buffered hydrofluoric acid for 1 min in order to remove the native oxide on the silicon surface, and then were rinsed in deionized water. The wafers were kept dry using a nitrogen gun, and immediately loaded into the prepurged quartz tube for nitridation. During the nitridation, the flow rate of ammonia gas was kept at

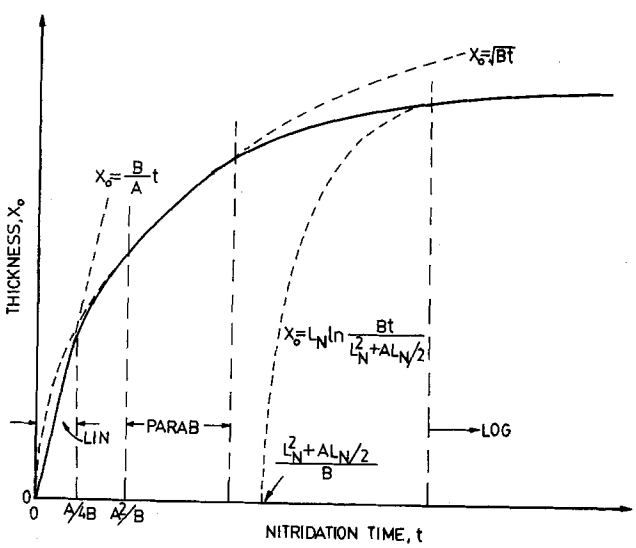


**Fig. 2. Typical nitridation time dependence of the as-grown thermal nitride film thickness.**

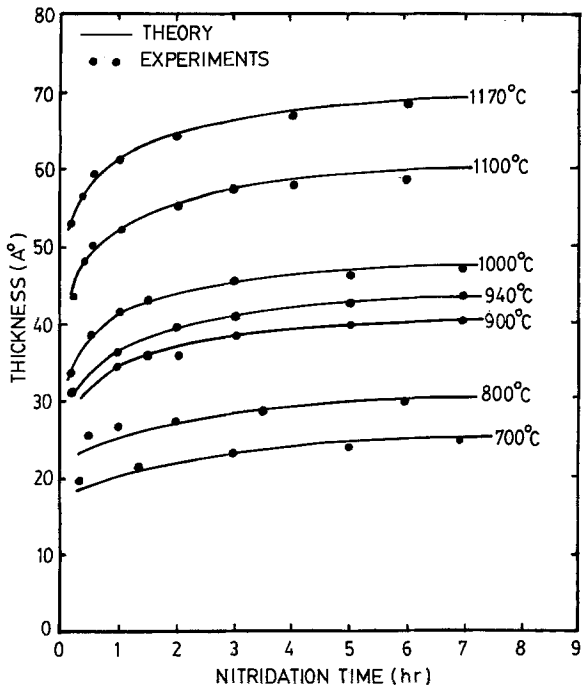


**Fig. 3. Comparisons between the growth rate data of the as-grown thermal nitride films and the theoretical model.**

about 400 cm³/min. The thickness of the fabricated thermal nitride films were measured by an ellipsometer. Figure 3 shows the thickness of the as-grown thermal nitride films as a function of nitridation time in ammonia gas for nitridation temperature from 700° to 1200°C, which indicates an initial rapid growth followed by an inhibited growth. Comparisons between the experimental data and the developed model are also shown in Fig. 3 and the parameters used are listed in Table I. It is clearly seen that good agreement between the experimental results and the theoretical calculations is obtained. Moreover, the characteristic diffusion length of the nitridant species across the thermal nitride film is shown to be smaller than 10Å for the nitridation temperature below 1200°C. Figure 4 shows the linear rate constant $B/A$ as a function of the inverse temperature, which gives the activation energy of about 1.286 eV. Note that the activation energy of the linear rate constant for the thermal nitridation is much smaller than that of the thermal oxidation ($E_a$ = 2.0 eV for dry $O_2$ oxidation). The main reason for smaller activation energy during the initial nitridation is mainly due to slow surface reaction between the nitridant species and the silicon surface. Similarly, the parabolic rate constant $B$ as a function of the inverse temperature is shown in Fig. 5, in which the activation energy is estimated to be about 1.546 eV. Figure 6 shows the characteristic diffusion length as a function of the inverse temperature which gives the activation energy of about 0.181 eV. It is clearly visualized that the logarithmic region of the thermal nitride growth is mainly due to the limited diffusion of the nitridant species across the thermal nitride film rather than due to the surface reaction between the nitridant species and the silicon surface. From the

**Table I. The characteristic parameters used to calculate the theoretical curves shown in Fig. 3**

| PARAMETERS / TEMPERATURE | DIFFUSION LENGTH $L_N$ (Å) | PARABOLIC RATE CONSTANT B ($\mu^2$/hr) | LINEAR RATE CONSTANT B/A ($\mu$/hr) |
|---|---|---|---|
| 1170°C | 5.049 | $4.717\times10^{-2}$ | 168.5 |
| 1100°C | 4.671 | $1.864\times10^{-2}$ | 69.94 |
| 1000°C | 4.152 | $8.141\times10^{-3}$ | 35.4 |
| 940°C | 3.699 | $3.531\times10^{-3}$ | 16.81 |
| 900°C | 3.607 | $2.046\times10^{-3}$ | 11.16 |
| 800°C | 3.071 | $4.832\times10^{-4}$ | 3.35 |
| 700°C | 2.454 | $2.169\times10^{-4}$ | 2.01 |

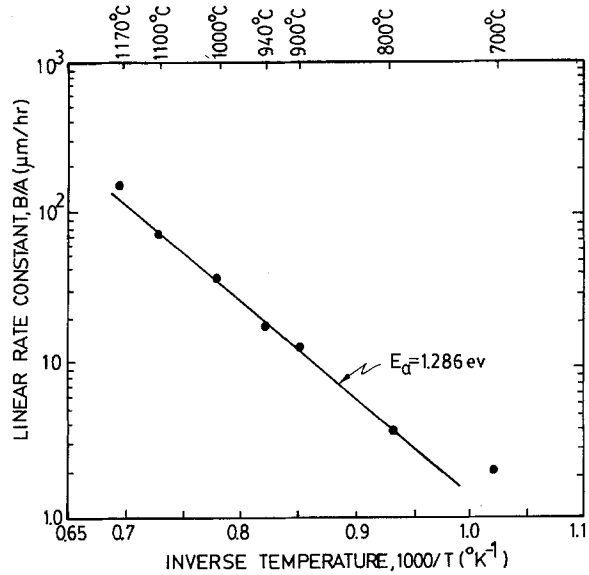


**Fig. 4. The measured linear growth rate constant of the as-grown thermal nitride films as a function of the inverse temperature.**

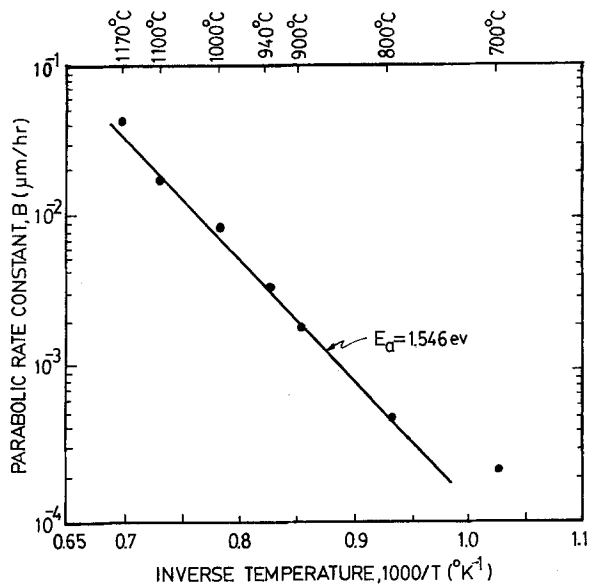


**Fig. 5. The measured parabolic growth rate constant of the as-grown thermal nitride films as a function of the inverse temperature.**

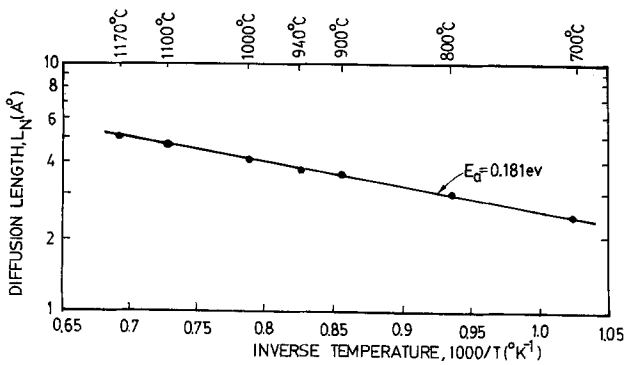


**Fig. 6. The measured characteristic diffusion length of the nitridant species across the as-grown thermal nitride films as a function of the inverse temperature.**

estimated activation energy, we may conclude that the reaction between the silicon wafer and the ammonia gas is slow and the as-grown thermal nitride films do have higher structure density than that of the thermally grown silicon dioxide.

## Conclusions

An analytical model for the growth kinetics of silicon thermal nitridation has been developed and compared to the experimental data. The characteristic parameters of silicon nitridation in ammonia gas, such as the linear rate constant, the parabolic rate constant, and the diffusion length of the nitridant species across the thermal nitride film, have been deduced and characterized. It has been shown that the diffusion length of the nitridant species across the thermal nitride film is smaller than 10Å when the nitridation temperature is below 1200°C. In addition, the self-limiting growth property of the silicon thermal nitridation in nitrogen or ammonia is shown mainly due to the shorter characteristic diffusion length of the nitridant species across the as-grown thermal nitride films which have higher structure density.

## Acknowledgment

The authors would like to express their sincere thanks to Dr. D. H. Hu and Dr. C. T. Shih of the Electronics Research and Service Organization, Industrial Technology Research Institute (ITRI) for their grant support and stimulating discussions. Special thanks to all the technical staff of Semiconductor Research Center, National Chiao-Tung University for their assistance during the experimental studies.

Manuscript received Sept. 9, 1981.

Any discussion of this paper will appear in a Discussion Section to be published in the June 1983 JOURNAL. All discussions for the June 1983 Discussion Section should be submitted by Feb. 1, 1983.

*Publication costs of this article were assisted by the National Chiao-Tung University.*

## REFERENCES

1. F. K. Heumann, D. M. Brown, and E. Mets, *This Journal*, **115**, 331 (1968).
2. S. M. Hu, *ibid.*, **113**, 693 (1966).
3. R. G. Frieser, *ibid.*, **115**, 1092 (1968).
4. S. I. Raider, R. A. Gdula, and J. R. Petrak, *ibid.*, **27**, 150 (1975).
5. E. Kooi, J. G. Van Lierop, and J. A. Appels, *ibid.*, **123**, 1117 (1976).
6. T. Ito, S. Hijiya, T. Nozaki, H. Arakawa, M. Shinoda, and Y. Fukukawa, *ibid.*, **125**, 448 (1978).
7. T. Ito, T. Nozaki, H. Arakawa, and M. Shinoda, *Appl. Phys. Lett.*, **32**, 330 (1978).
8. S. P. Murarka, C. C. Chang, and A. C. Adams, *This Journal*, **126**, 996 (1979).

# Doping of $Ga_{1-x}Al_xAs$ Grown by LPE with Si and Ge

**V. Swaminathan,* M. D. Sturge, J. L. Zilko, N. E. Schumaker,* and W. R. Wagner**

*Bell Laboratories, Murray Hill, New Jersey 07974*

**and C. A. Gaw**

*Bell Laboratories, Reading, Pennsylvania 19604*

## ABSTRACT

The electrical and optical properties of p-type Ge and Si-doped $Ga_{1-x}Al_xAs$ ($x \sim 0.39$-$0.42$) layers grown by liquid phase epitaxy in an He ambient have been investigated as a function of the atom fraction of Si in the melt, $X_{Si}$. For $X_{Si}$ in the range $1.5 \times 10^{-5}$ to $1.5 \times 10^{-2}$ the hole concentration at room temperature is relatively unaffected while the hole mobility decreases monotonically with addition of Si, suggesting close compensation of Si species. As a result, in the low temperature photoluminescent spectra, the pair transition via the shallow Si acceptors is quenched relative to that via the deep $Ge_{As}$ centers. For $X_{Si} < 5 \times 10^{-5}$, adding 0.9 ppm $O_2$ to the growth ambient decreases the compensation due to the removal of the background S donor, and thereby increases the hole concentration by a factor of 2-3 and enhances the pair transition via the Si acceptors as well. The addition of $O_2$ during LPE growth is not, however, always practical as it has been found to affect the uniformity of thin epitaxial layers.

Germanium (1) is frequently used as a p-type dopant in the $Ga_{1-x}Al_xAs$ ($x \sim 0.40$) cladding layer of the GaAs-(GaAl)As double heterostructure (DH) grown by liquid phase epitaxy (LPE) for the fabrication of injection lasers, and is preferred over other acceptor dopants like Be, Zn, or Cd which have either hazardous properties (Be), high diffusivity (Zn) (2), or low solubility (Cd) (3). The use of Ge is, however, not without its problems. High conductivity in the p-cladding layer is often desired for efficient confinement of carriers in the lasing active region and for reduced temperature dependence of the current threshold (4, 5). Increasing the Ge doping level to achieve high conductivities in the ternary decreases the aluminum segregation coefficient and radiative efficiency (6). Another approach to increase the conductivity would be to add a second acceptor dopant in the layer with Ge. Silicon might be thought to be a good candidate for this purpose since it has been reported to be a p-type dopant for growth under LPE conditions at temperatures below 800°C (7); it gives rise to a shallower acceptor level than Ge (8) and its segregation coefficient in (GaAl)As is at least an order of magnitude higher than Ge (6, 7). In this paper we report the results of adding varying amounts of Si in the range $10^{-4}$ to 1.5 atomic percent (a/o) to the LPE growth solution containing $5.5 \times 10^{-1}$ a/o of Ge and $2 \times 10^{-1}$ a/o of Al (for $x \sim 0.4$ in the solid). We find that addition of Si does not result in increased conductivity indicating that Si, which is amphoteric, is closely self-compensated in the solid under our growth conditions. This compensation also manifests itself in reduced low temperature photoluminescent intensities of pair transitions involving Si acceptors, relative to those involving Ge. An increase in the conductivity by a factor of 2-3 is observed when small amounts of $O_2$ are added to the generally used He growth ambient, for Si doping less than $5 \times 10^{-3}$ a/o. However, the use of $O_2$ during LPE growth of (GaAl)As DH structures is

* Electrochemical Society Active Member.

Key words: photoluminescence, Hall measurements, compensation.